

## RECENT RESULTS FROM HIGH-TEMPERATURE LATTICE QCD

*E. Laermann*\*

Faculty of Physics, Bielefeld University, Bielefeld, Germany

Recent results obtained from numerical computations in lattice regularized QCD are summarized. The write-up of the talk concentrates on the liberation of strange quarks in the vicinity of the chiral QCD transition and on certain ratios of cumulants of net electric charge fluctuations which can be used to determine freeze-out parameters by a comparison of experimental data from heavy-ion collisions with lattice QCD results.

PACS: 12.38.-t; 12.38.Gc

### INTRODUCTION

Fluctuations and correlations of conserved charges, like baryon number  $B$ , electric charge  $Q$ , or strangeness  $S$ , are sensitive to the composition of hot and dense QCD matter [1,2]. Measures of them in general take quite different values in a phase where the carriers of the quantum numbers are hadrons, opposed to a phase where those are quarks. It is therefore of interest to compute fluctuation and correlation quantities from QCD to study the properties of strong-interaction matter at high temperature and density.

Moreover, fluctuations measured in a heavy-ion collision experiment may reflect thermal conditions at the time where the generated medium has expanded, cooled down, and diluted sufficiently, so that hadrons form again. Although it may be questioned whether the thermal medium at this time is in equilibrium and how well hadronization is localized in time, the success of hadron resonance gas (HRG) model calculations, performed to describe properties of the medium at the time of freeze-out [3], seems to suggest that the thermal conditions are well characterized by a freeze-out temperature  $T_f$  and a baryon chemical potential  $\mu_B^f$ . The values  $T_f$  and  $\mu_B^f$  at freeze-out are usually determined by comparing experimental data on particle yields with a HRG model calculation [3,4]. However, it is clearly

---

\*E-mail: edwin@physik.uni-bielefeld.de

desirable to extract the freeze-out parameters also by comparing experimental data directly with a QCD calculation.

In the following write-up of the talk we will concentrate on strangeness liberation and on determining freeze-out parameters with the help of lattice QCD. Both topics rely on our measurements of fluctuation and correlation variables performed for two degenerate light quarks and a strange quark. The quark mass values have been tuned such that the kaon mass acquires its physical value and that the (Goldstone) pion is of mass 160 MeV. The simulations are based on the so-called HISQ action [5] for the quarks, a highly improved discretization with small discretization errors (taste violations). At aspect ratios  $N_\sigma/N_\tau \geq 4$ , the temporal extents of the  $N_\sigma^3 \times N_\tau$  lattices have been chosen as  $N_\tau = 6, 8$ , and 12 to address finite lattice spacing effects  $\sim (N_\tau T)^{-1}$  with  $T$  being the temperature.

## 1. STRANGENESS LIBERATION

The basic quantities calculated on the lattice arise from the Taylor expansion of the pressure, or equivalently of the logarithm of the partition function,

$$\frac{p}{T^4} = \frac{1}{VT^3} \ln Z(T, \mu_u, \mu_d, \mu_s) = \sum_{i,j,k} \frac{1}{i!j!k!} \chi_{ijk}(T) \left(\frac{\mu_u}{T}\right)^i \left(\frac{\mu_d}{T}\right)^j \left(\frac{\mu_s}{T}\right)^k$$

with respect to the quark chemical potentials  $\mu_{u,d,s}$ . The expansion coefficients  $\chi_{ijk}$  are computed at vanishing chemical potentials and are readily combined into generalized susceptibilities\*  $\chi_{ijk}^{BQS}$  which are related to correlations between the conserved quantum numbers  $B, Q$ , and  $S$ , as well as to cumulants of fluctuations like, e.g., variance, skewness, or kurtosis.

The generalized susceptibilities can also be obtained in hadron resonance gas model calculations. In a HRG picture the contribution to the partition function  $Z$  of a meson ( $M$ ) or a baryon ( $B$ ) with quantum numbers and mass indexed by  $i$  is given by

$$\ln Z_i^{M/B} \sim \sum_{k=1}^{\infty} \frac{(\pm 1)^{k+1}}{k^2} K_2\left(\frac{km_i}{T}\right) \cosh(k(B_i \hat{\mu}_B + Q_i \hat{\mu}_Q + S_i \hat{\mu}_S)) \quad (1)$$

( $\hat{\mu}_X = \mu_X/T$ ,  $X = B, Q, S$ ), such that the total pressure is obtained as a sum over of partial pressures  $M_{|S|}$  and  $B_{|S|}$  of mesons and baryons, respectively,

$$\begin{aligned} \frac{p}{T^4} &= M_0(T) + M_1(T) \cosh(-\hat{\mu}_S) + B_0(T) \cosh(\hat{\mu}_B) + \\ &+ B_1(T) \cosh(\hat{\mu}_B - \hat{\mu}_S) + B_2(T) \cosh(\hat{\mu}_B - 2\hat{\mu}_S) + B_3(T) \cosh(\hat{\mu}_B - 3\hat{\mu}_S), \end{aligned} \quad (2)$$

---

\*Whenever a subscript is zero it will be omitted as is the corresponding superscript.

where for the strange mesons and the baryons the Boltzmann approximation has been applied which is good within 2% accuracy. Taking Eq. (2) as a starting point for HRG computations of  $\chi_{ijk}^{BQS}$  as appropriate derivatives with respect to the chemical potentials, it is easily seen that in a gas of uncorrelated hadrons  $\chi_2^B = \chi_4^B$ , for instance, whereas the deviation of  $\chi_4^S$  from  $\chi_2^S$  is a measure for the contribution of  $|S| > 1$  hadrons. This contribution is shown in Fig. 1 to be quite substantial below the chiral crossover at  $T = 154(9)$  MeV [6] indicated as the grey band. At higher temperature though, the ratio of the susceptibilities  $\chi_4^S/\chi_2^S$  rapidly approaches the free quark gas value.

Up to fourth order in the derivative with respect to the strangeness chemical potential, in a hadron resonance gas, Eq. (2), there are six generalized susceptibilities,  $\chi_{11}^{BS}$ ,  $\chi_{31}^{BS}$ ,  $\chi_2^S$ ,  $\chi_{22}^{BS}$ ,  $\chi_{13}^{BS}$ , and  $\chi_4^S$ , but only four partial pressures. Thus one can construct two independent combinations of the susceptibilities that should vanish in a phase where the  $B$  and  $S$  quantum numbers are carried by hadrons, e.g.,

$$\begin{aligned} v_1 &= \chi_{31}^{BS} - \chi_{11}^{BS}, \\ v_2 &= \frac{1}{3}(\chi_2^S - \chi_4^S) - 2\chi_{13}^{BS} - 4\chi_{22}^{BS} - 2\chi_{31}^{BS}. \end{aligned} \quad (3)$$

These quantities are also shown in Fig. 1. As can be seen,  $v_1$  and  $v_2$  are vanishing up to temperatures in the chiral transition range, in accord with the hadron gas scenario, but simultaneously rise rapidly beyond. This rise is comparable in size to the rise in  $\chi_2^B - \chi_4^B$  shown in Fig. 1, *c*. This fact shows that the behavior of the strange degrees of freedom is very similar to the one of light quarks. Both sets of quantities are approaching the predictions of resummed Hard Thermal Loop (HTL) perturbation theory [7] at temperatures of about two times the chiral crossover one\*.

Solving for the partial pressures  $M_{|S|}$  and  $B_{|S|}$  arising from the strange hadron sector ( $|S| \geq 1$ ) of an HRG leads to

$$\begin{aligned} M_1(c_1, c_2) &= \chi_2^S - \chi_{22}^{BS} + c_1 v_1 + c_2 v_2, \\ B_1(c_1, c_2) &= \frac{1}{2}(\chi_4^S - \chi_2^S + 5\chi_{13}^{BS} + 7\chi_{22}^{BS}) + c_1 v_1 + c_2 v_2, \\ B_2(c_1, c_2) &= -\frac{1}{4}(\chi_4^S - \chi_2^S + 4\chi_{13}^{BS} + 4\chi_{22}^{BS}) + c_1 v_1 + c_2 v_2, \\ B_3(c_1, c_2) &= \frac{1}{18}(\chi_4^S - \chi_2^S + 3\chi_{13}^{BS} + 3\chi_{22}^{BS}) + c_1 v_1 + c_2 v_2, \end{aligned} \quad (4)$$

---

\*For a more detailed discussion, see [8].

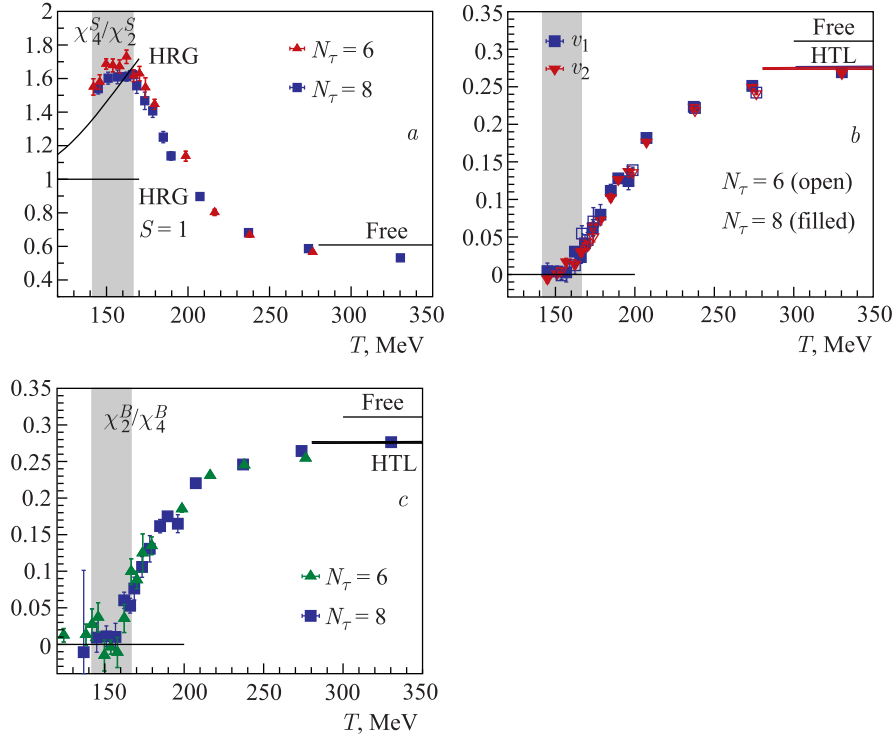


Fig. 1. The quantities  $\chi_4^S / \chi_2^S$  (a),  $v_1$  and  $v_2$  of Eq. (3) (b), and  $\chi_2^B - \chi_4^B$  (c) as a function of temperature. The grey bands indicate the chiral transition region

where arbitrary linear combinations of  $v_1$  and  $v_2$  can be added without affecting the result. These partial pressures are shown in Fig. 2. While at low temperatures up to the chiral transition region the various linear combinations agree with each other and with the HRG predictions, the hadronic description of the strange degrees of freedom breaks down just above  $T_c$ .

## 2. FREEZE-OUT PARAMETERS

As mentioned in the previous section, the lattice results for generalized susceptibilities depend on temperature and the chemical potentials  $\mu_B$ ,  $\mu_Q$ , and  $\mu_S$ . In order to get access to the freeze-out parameters  $T_f$  and  $\mu_B^f$ , one needs to fix  $\mu_Q$  and  $\mu_S$  to the values that characterize a thermal system created in a heavy-ion collision. These values are determined by assuming that the thermal subvolume, probed by measuring fluctuations in a certain rapidity and transverse momentum

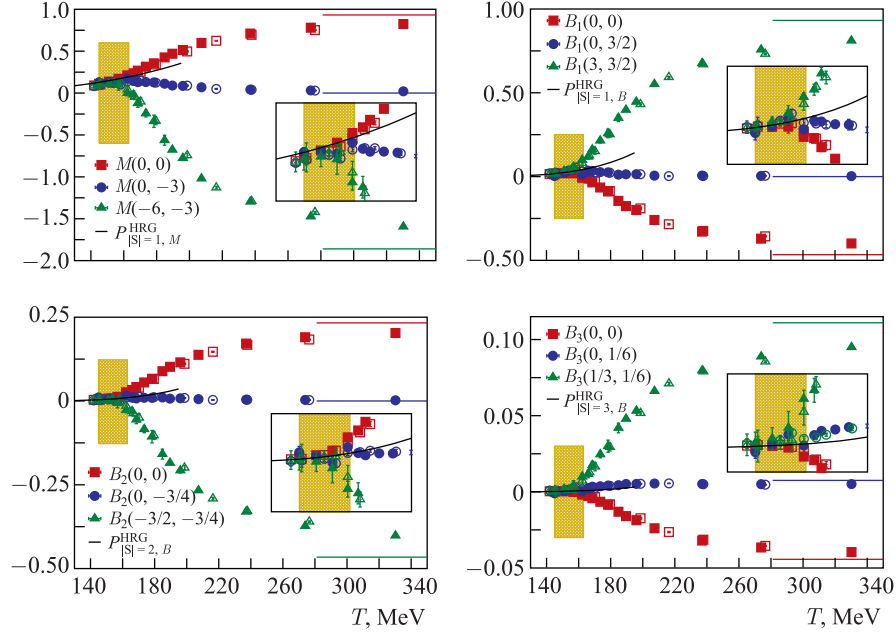


Fig. 2 (color online). Partial pressures arising from the strange sector of an HRG, Eq. (4). The yellow bands indicate the chiral transition region, whereas the colored lines on the right side denote the quark gas values

window, reflects the net strangeness content and electric charge to baryon number ratios of the incident nuclei,

$$\langle n_S \rangle = 0, \quad \langle n_Q \rangle = r \langle n_B \rangle, \quad (5)$$

where  $r$  is approximately 0.4 for Au–Au as well as Pb–Pb collisions. Expanding the densities in terms of the chemical potentials, one can solve for  $\mu_Q$  and  $\mu_S$  order by order in the expansion, with the result up to the next-to-leading order (NLO) as

$$\hat{\mu}_Q = q_1 \hat{\mu}_B + q_3 \hat{\mu}_B^3, \quad \hat{\mu}_S = s_1 \hat{\mu}_B + s_3 \hat{\mu}_B^3. \quad (6)$$

The leading order expansion coefficients for  $\hat{\mu}_Q$  and  $\hat{\mu}_S$  are shown in the top panels of Fig. 3. Based on spline interpolations of the numerical results obtained for three different lattice sizes, extrapolations to the continuum limit were carried out using an ansatz linear in  $1/N_\tau^2$ . The resulting extrapolations are shown as bands in these panels. In order to check the importance of NLO corrections,  $s_3$  and  $q_3$  were calculated on lattices with temporal extent  $N_\tau = 6$  and 8. The results, expressed in units of the leading order terms, are also shown in Fig. 3.

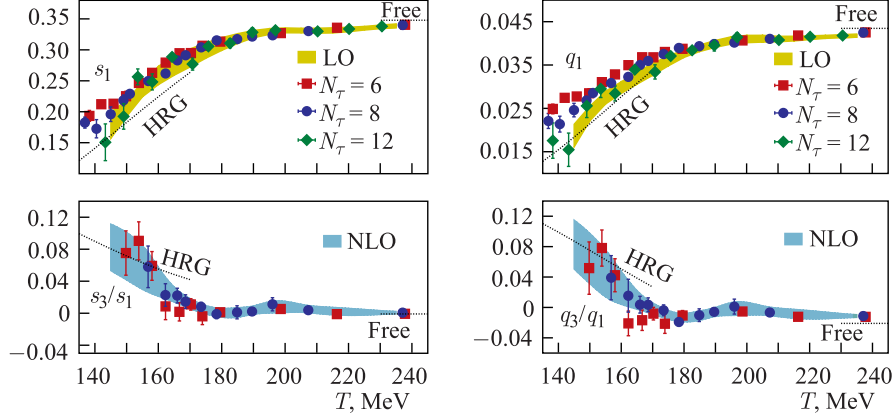


Fig. 3. The leading and next-to-leading order expansion coefficients of the strangeness (left) and the negative of the electric charge chemical potentials (right) versus temperature for  $r = 0.4$ . For  $s_1$  and  $q_1$  the LO-bands show results for the continuum extrapolation. For  $s_3$  and  $q_3$  we give an estimate for continuum results (NLO bands) based on spline interpolations of the  $N_\tau = 8$  data. Dashed lines at low temperature are from the HRG model and at high temperature from a massless, 3-flavor quark gas

It is obvious from this figure that NLO corrections indeed are negligible in the high-temperature region and smaller than 10% in the temperature interval relevant for the analysis of freeze-out conditions, i.e.,  $T \simeq (160 \pm 10)$  MeV. For a more detailed discussion of the errors of these and other quantities presented below, we refer to [9].

Having thus adjusted the values for  $\mu_Q$  and  $\mu_S$  to the physical conditions met in a heavy-ion collision, two further quantities are needed to fix  $T^f$  and  $\mu_B^f$ . Of particular interest are ratios of cumulants which to a large extent eliminate the dependence of cumulants on the freeze-out volume. Since only proton instead of baryon fluctuations are available experimentally, electric charge fluctuations appear to be most appropriate. The simplest of such ratios involve mean  $M_Q$ , variance  $\sigma_Q^2$ , and skewness  $S_Q$ . Those can be combined to

$$\frac{M_Q(s)}{\sigma_Q^2(s)} = \frac{\chi_1^Q(T, \mu_B)}{\chi_2^Q(T, \mu_B)} = R_{12}^Q(T, \mu_B) = R_{12}^{Q,1}(T) \hat{\mu}_B + R_{12}^{Q,3}(T) \hat{\mu}_B^3 + \dots, \quad (7)$$

$$\frac{S_Q(s) \sigma_Q^3(s)}{M_Q(s)} = \frac{\chi_3^Q(T, \mu_B)}{\chi_1^Q(T, \mu_B)} = R_{31}^Q(T, \mu_B) = R_{31}^{Q,0}(T) + R_{31}^{Q,2}(T) \hat{\mu}_B^2 + \dots \quad (8)$$

These ratios can be computed in QCD (as well as in the HRG model) and compared to experimental data in order to determine  $T^f$  and  $\mu_B^f$ . We evaluated

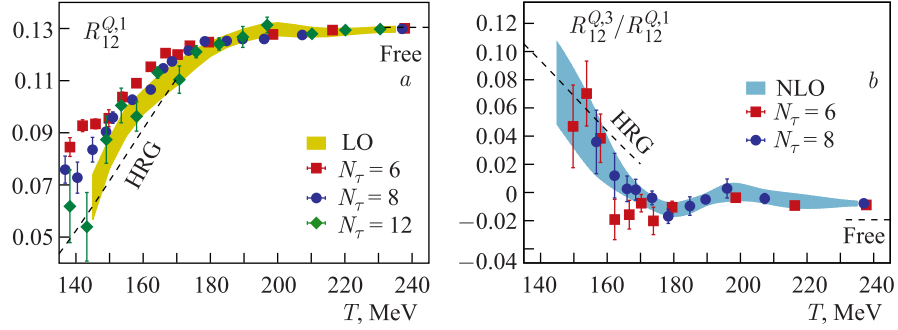


Fig. 4. The leading (a) and next-to-leading (b) order expansion coefficients of the ratio of first- to second-order cumulants of net electric charge fluctuations versus temperature for  $r = 0.4$ . The bands and lines are the same as in Fig. 3

them to leading order for  $R_{31}^Q$  and up to  $\mathcal{O}(\hat{\mu}_B^3)$  for  $R_{12}^Q$ . For the latter case the leading order and the NLO corrections are shown in Fig. 4. The LO results have been obtained on lattices with  $N_\tau = 6, 8$ , and  $12$ . They show small discretization effects and were extrapolated to the continuum limit. The NLO corrections to the ratio of electric charge cumulants are below 10%, which makes the leading order result a good approximation for a large range of  $\hat{\mu}_B$ .

The leading part of the ratio  $R_{12}^Q$  depends linearly on  $\mu_B$  such that this ratio has a strong dependence on  $\mu_B$ , but varies little with  $T$  for  $T \simeq (160 \pm 10)$  MeV, see Fig. 5, a. On the contrary, the leading order  $R_{31}^Q$  depends strongly on  $T$ , Fig. 5, b, and shows a characteristic temperature dependence for  $T \gtrsim 155$  MeV that is quite different from that of HRG model calculations. It receives corrections only at  $\mathcal{O}(\hat{\mu}_B^2)$  an estimate of which has been added as blueish band in this figure.

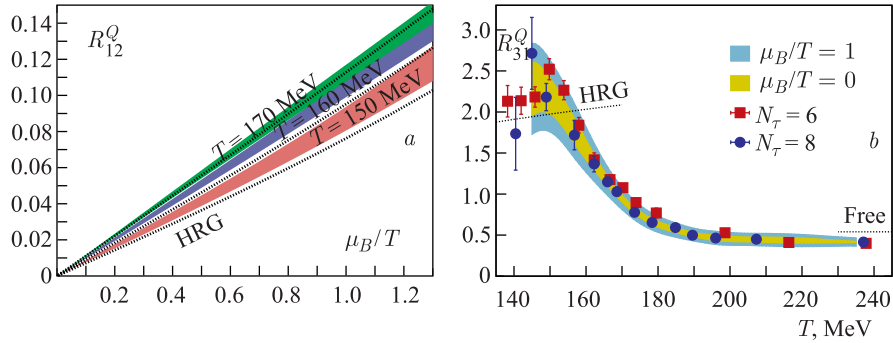


Fig. 5 (color online). The ratios  $R_{12}^Q$  versus  $\mu_B/T$  (a) for three values of the temperature and  $R_{31}^Q$  versus temperature for  $\mu_B = 0$  (b). The wider band on the data set for  $N_\tau = 8$  (b) shows an estimate of the magnitude of NLO corrections at  $\mu_B/T = 1$

The idea is now to compare the lattice results for these ratios, which are functions of  $T$  and  $\mu_B$ , to experimental data at given center-of-mass energy. A measurement of  $R_{31}^Q$  lends itself for a determination of the freeze-out temperature, with small values of  $R_{31}^Q$  favoring large freeze-out temperatures  $T^f$  and vice versa. Subsequently, a comparison of experimental data on  $R_{12}^Q$  with Fig. 5, *b* will allow one to determine  $\mu_B^f$ .

## CONCLUSIONS

The lattice QCD results presented here show that up to the chiral crossover temperature  $T_c$  the quantum numbers associated with strange degrees of freedom are consistent with that of an uncorrelated gas of hadrons. The lattice results also show that such a hadronic description breaks down just above  $T_c$ . Moreover, the behavior of the strange degrees of freedom around  $T_c$  is quite similar to that involving the light up and down quarks, altogether suggesting that the deconfinement of strangeness takes place at the chiral crossover temperature.

Furthermore, the first three cumulants of net electric charge fluctuations are well suited for a determination of freeze-out parameters in a heavy-ion collision. Although the ratios  $R_{12}^Q$  and  $R_{31}^Q$  are sufficient to determine  $T_f$  and  $\mu_B^f$ , it would be advantageous to have several ratios to probe the consistency of an equilibrium thermodynamic description of freeze-out. When comparing these results to experimental data, one will however need to take into account the details of the actual experimental setup. In addition, the thermodynamic relevance of additional, experimentally yet unobserved strange baryons, as observed in the meantime after the Symposium [10], also has consequences for the analysis of freeze-out conditions in heavy-ion experiments.

**Acknowledgements.** The author is grateful to organizers for the outstanding atmosphere at the Symposium. The presentation here is based on work within the BNL–Bielefeld collaboration. Partial financial support from the European Union under grant agreement No. 238353 is acknowledged.

## REFERENCES

1. Koch V., Majumder A., Randrup J. Baryon-Strangeness Correlations: A Diagnostic of Strongly Interacting Matter // Phys. Rev. Lett. 2005. V. 95. P. 182301.
2. Ejiri S., Karsch F., Redlich K. Hadronic Fluctuations at the QCD Phase Transition // Phys. Lett. B. 2006. V. 633. P. 275.
3. Braun-Munzinger P., Redlich K., Stachel J. Particle Production in Heavy-Ion Collisions // Quark Gluon Plasma / Ed. Hwa R. C. et al. P. 491; nucl-th/0304013.
4. Cleymans J. et al. Comparison of Chemical Freeze-Out Criteria in Heavy-Ion Collisions // Phys. Rev. C. 2006. V. 73. P. 034905.

5. *Follana E. et al. (HPQCD and UKQCD Collabs.). Highly Improved Staggered Quarks on the Lattice, with Applications to Charm Physics // Phys. Rev. D. 2007. V. 75. P. 054502.*
6. *Bazavov A. et al. The Chiral and Deconfinement Aspects of the QCD Transition // Phys. Rev. D. 2012. V. 85. P. 054503.*
7. *Andersen J. O., Mogliacci S., Su N., Vuorinen A. Quark Number Susceptibilities from Resummed Perturbation Theory // Phys. Rev. D. 2013. V. 87. P. 074003.*
8. *Bazavov A. et al. Strangeness at High Temperatures: From Hadrons to Quarks // Phys. Rev. Lett. 2013. V. 111. P. 082301.*
9. *Bazavov A. et al. Freeze-Out Conditions in Heavy-Ion Collisions from QCD Thermodynamics // Phys. Rev. Lett. 2012. V. 109. P. 192302.*
10. *Bazavov A. et al. Additional Strange Hadrons from QCD Thermodynamics and Strangeness Freeze-Out in Heavy-Ion Collisions // Phys. Rev. Lett. 2014. V. 113. P. 072001.*